

Magnetic phase transitions in $RFe_{10}Mo_2$ compounds

This article has been downloaded from IOPscience. Please scroll down to see the full text article.

1993 J. Phys.: Condens. Matter 5 8611

(<http://iopscience.iop.org/0953-8984/5/45/014>)

View [the table of contents for this issue](#), or go to the [journal homepage](#) for more

Download details:

IP Address: 171.66.16.96

The article was downloaded on 11/05/2010 at 02:14

Please note that [terms and conditions apply](#).

Magnetic phase transitions in $RFe_{10}Mo_2$ compounds

C Christides†, A Kostikas†, X C Kou‡, R Grossinger‡ and D Niarchos†

† National Centre for Scientific Research 'Demokritos', Institute of Materials Science, 153 10 Ag, Paraskevi, Attiki, Greece

‡ Institute für Experimentalphysik, Technische Universität Vienna, A-1040 Vienna, Austria

Received 14 July 1993, in final form 11 August 1993

Abstract. A variety of magnetic phase transitions have been observed for all the $RFe_{10}Mo_2$ compounds from AC and DC magnetic measurements in the temperature range between 4.2 and 300 K. The alloys with $R = Nd, Tb$ and Dy exhibit spin reorientation transitions and with $R = Ho, Er$ and Tm some unidentified magnetic phase transitions occur which are accompanied by strong relaxation effects in the ^{57}Fe Mössbauer spectra of $TmFe_{10}Mo_2$. The observed magnetic transitions may be broadly interpreted in terms of a mean-field mixed-exchange model, although the detailed behaviour is somewhat different.

1. Introduction

The relatively high Curie temperatures T_C and magnetizations M_s observed for the intermetallic compounds with the general formula $RFe_{12-x}T_x$ ($T = Ti$ or W , with $x = 1, 2$, and $T = V, Cr, Mo$ or Si with $x = 2$) and the uniaxial anisotropy of the tetragonal structure (ThMn₁₂ type) make these materials possible candidates as inexpensive alternatives for permanent magnets [1, 2]. The observation of magnetic phase transitions (i.e. spin reorientations (SRT) and first-order magnetization process (FOMP) gave rise to an extensive study of the magnetocrystalline anisotropy in these compounds [3, 4]. The contribution of extra states from transition-metal elements T into the 3d band of the Fe sublattice [5] has been considered to be responsible for the observed differences in the T_C and M_s values of the 1:12 compounds with the same R and different T [6]. The exceptionally low T_C and M_s -values observed for the $RFe_{10}Mo_2$ alloys in comparison with those observed for the rest of the $RFe_{12-x}T_x$ series [1] provide a strong indication of the high sensitivity of the iron sublattice band magnetism to the atomic environment and interaction distances. However, the appreciable 'spontaneous' coercive field B_c ($= 0.25$ T at 5 K) observed for $SmFe_{10}Mo_2$ as-cast material [1] led to a metallurgical investigation with the aim of direct application in permanent magnets [7]. Mechanical alloying has been used for the development of sufficient microstructure, in order to improve the energy product $(BH)_{max}$ of the as-cast $SmFe_{10}Mo_2$ material [7] which gave a maximum $B_c = 0.47$ T at RT. This B_c is considerably smaller than the coercive field of 1.1 T achieved in the processed materials with Sm–Fe–Ti or V [8], contrary to that expected from the approximately zero B_c observed in as-cast samples of single-phase 1:12 compounds with $T = Ti$ or V. The preparation of nitrogenated $RFe_{10}Mo_2N_x$ samples [9] produced a significant change in their magnetic properties which caused the Nd-based 1:12 materials to become possible candidates for direct application as permanent magnets [10]. In order to understand their intrinsic magnetic properties a detailed study of the non-nitrogenated $RFe_{10}Mo_2$ compounds is required.

Preliminary AC susceptibility measurements and results from the singular point detection (SPD) method are indicative of the existence of many magnetic phase transitions (MPTs) at low temperatures in the $R\text{Fe}_{10}\text{Mo}_2$ compounds [11, 21]. In this study we have focused our attention on the magnetic behaviour of these alloys.

2. Experimental details

Samples with the nominal composition $R\text{Fe}_{10}\text{Mo}_2$ ($R = \text{Y, Nd, Sm, Gd, Tb, Dy, Ho, Er, Tm}$ and Lu) and $\text{SmFe}_8\text{Co}_2\text{Mo}_2$ were prepared from 99.9% pure starting materials. After arc melting, the samples were vacuum annealed at 850 °C for 5 d. From the x-ray powder diffraction measurements (with a Siemens D500 diffractometer) the samples were found to be single phase with a tetragonal ThMn_{12} -type structure.

DC magnetic measurements as a function of temperature were performed in the temperature range between 5 and 500 K using a vibrating-sample magnetometer (PAR155) under the influence of a homogeneous field of 0.05 T. Isothermal magnetic curves of the powder polycrystalline samples were measured using a maximum field of 2 T at 5 K. Values of the saturation magnetization M_s were derived from the high-field part of the isotherm curves by extrapolation with the law of approach to saturation [13]. For the AC magnetic susceptibility measurements a field with an amplitude of 40 A m^{-1} (1 Oe) and frequency $f = 125$ Hz has been used. The SPD measurements, which are discussed below, are all part of previous experimental work [11, 20].

The ^{57}Fe Mössbauer spectra were recorded from 5 to 300 K for non-oriented $\text{TmFe}_{10}\text{Mo}_2$ absorbers using a conventional constant-acceleration spectrometer. The source consisted of ^{57}Co in Rh moving at RT while the absorber was kept fixed.

3. Magnetic measurements

The T_C and M_s -values obtained are plotted in figures 1 and 2 together with measured values for some other 1:12 series [1, 9, 14, 15] for comparison. Since the formation of alloys with the ThMn_{12} crystal structure for $R = \text{La}$ has not been achieved at present for any of the 1:12 reported stoichiometries, the magnetization of the yttrium-based compound has been used for comparison in figure 2. The Mo compounds present the lowest T_C (30%) and M_s (20%). In addition, small deviations (± 0.2) from the nominal stoichiometry $x = 2$ in $\text{GdFe}_{12-x}\text{Mo}_x$ alloys [12], with $T_C = 440$ K, causes variations of ± 60 K respectively in T_C . These are indications that in these compounds the exchange interactions are strongly affected by small changes in the ratio of Fe to Mo atoms and the Mo concentration seems to be responsible for the considerable compensation of their magnetic properties.

Because of the low T_C -values it was impossible to prepare oriented samples for thermomagnetic measurements parallel and perpendicular to the orientation axis for the compounds with heavy rare earths in order to be able to distinguish SRT from other MPTs. All the reported measurements were performed on non-oriented pulverized polycrystalline samples. DC thermomagnetic curves on powder samples are plotted in figure 3, only for the compounds which present some anomalies indicating a MPT. The thermal variation in the AC initial susceptibility χ' (real part) is presented in figure 4 for the alloys with $R = \text{Tb, Dy, Ho, Er}$ and Tm . From these measurements it is obvious that there are many MPTs which are different from those observed in the rest of the $R\text{Fe}_{10}\text{T}_2$ ($T = \text{V, Cr}$ and Si) compounds. The weakening of the iron sublattice magnetism from the substitution of Mo atoms seems

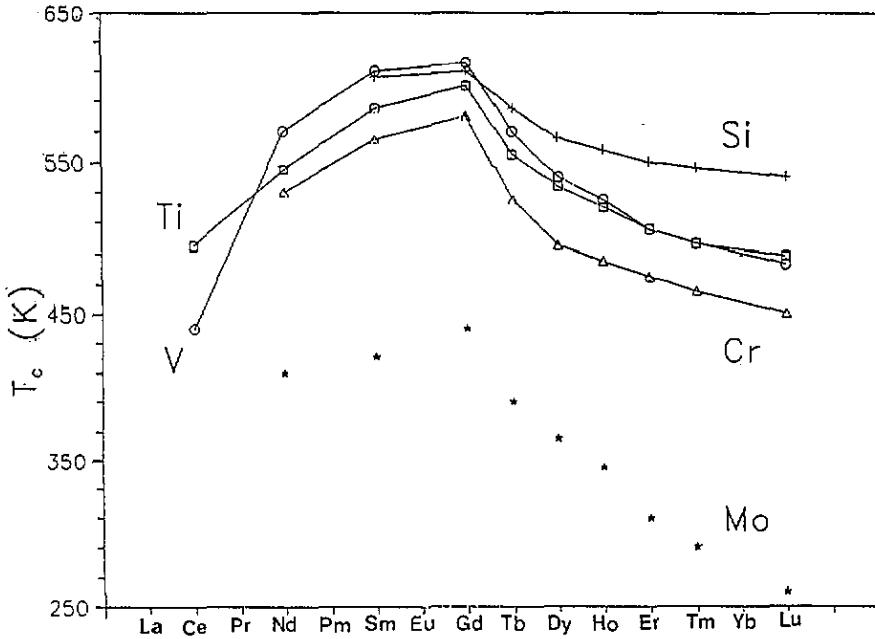


Figure 1. Observed magnetic ordering temperatures T_C from DC magnetic measurements on the $RFe_{12-x}T_x$ series of alloys ($T = Ti, x = 1$, and $T = V, Cr$ or $Mo, x = 2$).

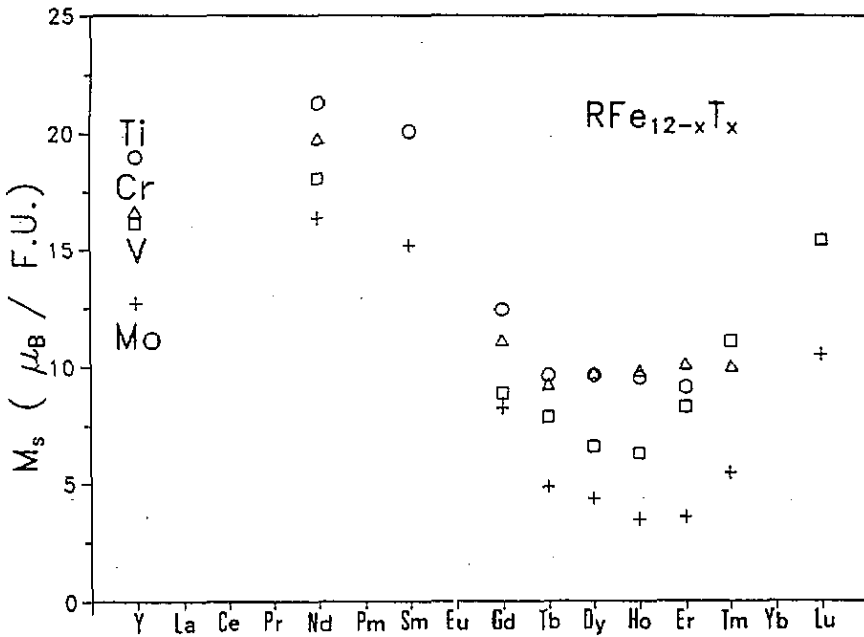


Figure 2. Observed magnetic moments M_s from DC magnetic measurements at 4.5 K ($T = Ti, x = 1$, and $T = V, Cr$ or $Mo, x = 2$).

to bring these alloys into a range of exchange interactions where the R-Fe coupling is the regulating term which affects the magnetic ordering significantly. Therefore, it is more convenient for the study of these compounds to separate them into two different groups according to the strength of magnetic interactions J (correlated to the critical temperature T_c) relative to thermal energy of the ambient:

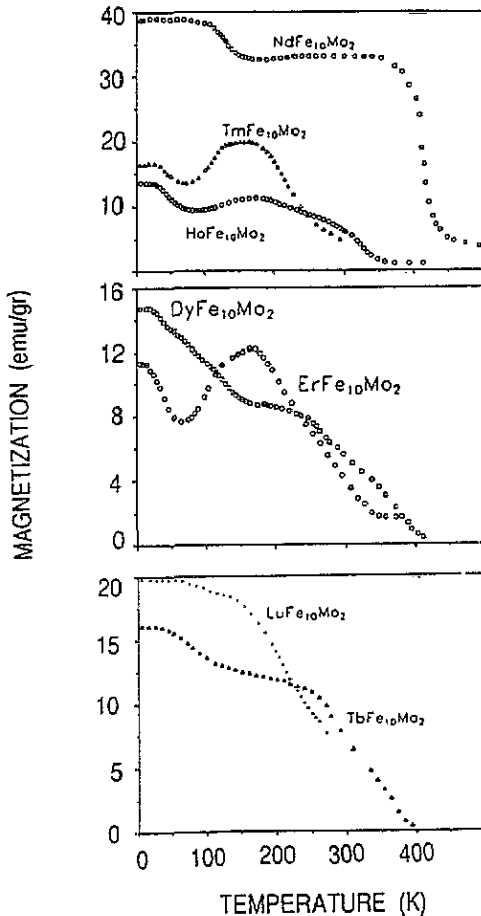


Figure 3. DC magnetic measurements as a function of temperature in a homogeneous applied magnetic field of 0.05 T.

3.1. Compounds with T_c values well above RT

3.1.1. $\text{SmFe}_{10}\text{Mo}_2$. A type II FOMP transition has been measured at 170 K [11] similar to that observed for $\text{SmFe}_{11}\text{Ti}$ [16]. We have measured a maximum coercive field of 0.26 T at 4.2 K, which is the same for the as-cast and annealed powder samples. The Co substitution in $\text{SmFe}_8\text{Co}_2\text{Mo}_2$ improves T_c ($= 490$ K) but reduces considerably the observed hysteresis loop at 5 K ($B_c = 0.08$ T).

3.1.2. $\text{NdFe}_{10}\text{Mo}_2$. A SRT occurs at approximately 140 K according to DC (figure 3) and AC (figure 4) magnetic susceptibility data as is expected for all the 1:12 compounds with a second-order Stevens coefficient $a_J < 0$ for the R^{3+} ion [3].

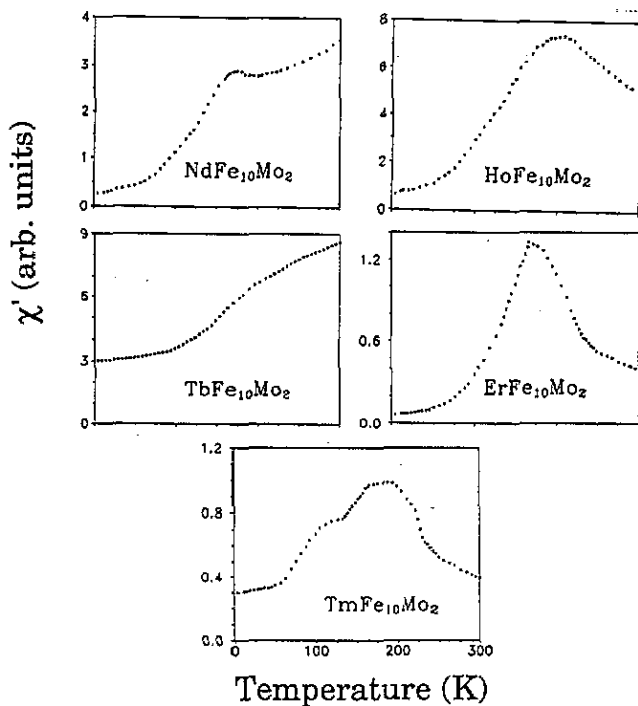


Figure 4. Variation in the real part χ' of the AC susceptibility as a function of temperature in a field with an amplitude of 40 A m^{-1} and a frequency of $f = 125 \text{ Hz}$.

3.1.3. $GdFe_{10}Mo_2$. There are no MPTs and the variation in the anisotropy field with temperature is smooth [21]. The coercive field is negligible for the whole temperature range examined.

3.1.4. $TbFe_{10}Mo_2$. The anisotropy field B_A is approximately half that observed for the Gd compound [11]. χ' versus T shows a smooth transition which is in agreement with the slope change observed for DC magnetic measurements. Since the Tb^{3+} ion has $a_J < 0$, the existence of a SRT of the magnetic vector from a direction of M_s out of the c axis at very low temperatures to a direction closer to this axis by increasing T could explain the very low B_A -values.

3.1.5. $DyFe_{10}Mo_2$. The AC, DC and SPD magnetic measurements as functions of T (figures 3 and 4) [11] are indicative of the appearance of a first-order SRT at 150 K which turns the magnetic moments perpendicular to the c axis at low T .

3.2. Compounds with T_C values compared to RT

3.2.1. $HoFe_{10}Mo_2$. Two transitions were observed in AC and DC thermomagnetic curves: one at 95 K and the other at 150 K. The origin of these MPTs is unidentified and the SPD measurements cannot provide any further information since it was impossible to detect SPD singularities.

3.2.2. $ErFe_{10}Mo_2$. For this sample the 'valley' between the two smooth peaks observed in DC magnetic measurements on the Ho compound becomes deeper and is accompanied by a considerable increase in the peak at higher temperatures. The AC susceptibility peak appears narrower than that of the Ho alloy, indicating a well defined transition temperature at 220 K. No SPD singularities were observed.

3.2.3. $TmFe_{10}Mo_2$. The χ' data show two well defined MPTs, which seem to be in agreement with the temperature range where the peaks observed from DC measurements start to increase on both sides of the 'valley'. Surprisingly, a remarkable coercive field of 0.32 T has been observed at 4.2 K after zero-field cooling (ZFC), and a shift in the hysteresis loop occurs with a field-cooling (FC) process (figure 5). The values of the remanent magnetization M_r and B_c observed for the $RFe_{10}Mo_2$ compounds which present a hysteresis loop at 5 K are listed in table 1 for the ZFC and FC measurements. Only for the alloys with $R = Tm$ and Lu has a shift in the hysteresis loop been observed. However, the absence of SPD singularities for the compounds with $R = Ho, Er$ and Tm is a strong indication that the anisotropy either is not uniaxial or is very low. Consequently, the observed hysteresis loops can be related to a special magnetic configuration of spins.

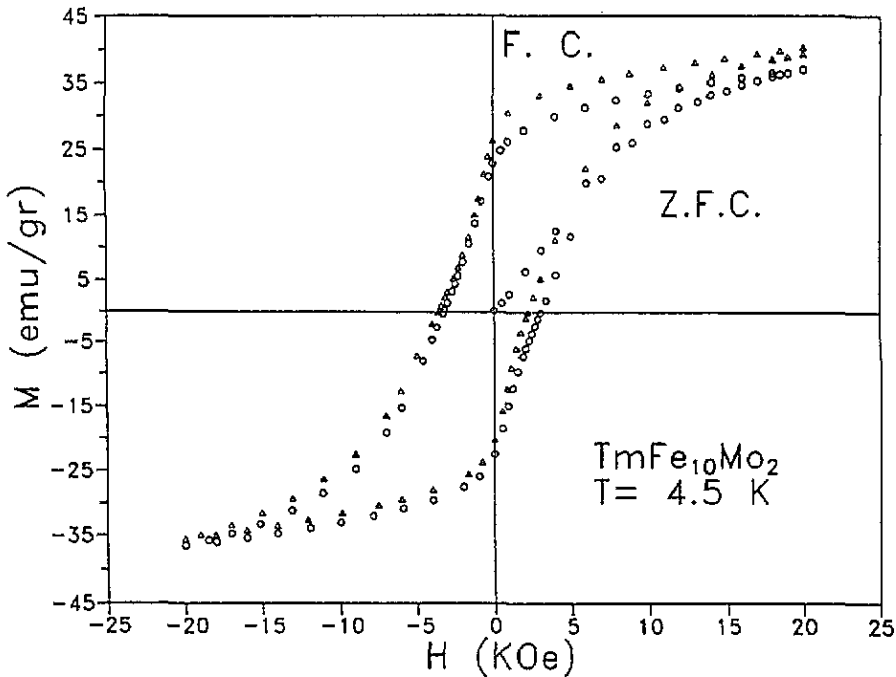


Figure 5. Hysteresis loops after ZFC and FC processes observed using a maximum applied magnetic field of 2 T.

For the compounds with $R = Y$ and Lu a variety of magnetic transitions have been detected using many different experimental techniques and their spin-glass-like magnetic properties have been reported in a separate study [21].

Table 1. Observed coercive fields B_c and remanent magnetization M_r after ZFC and FC hysteresis loop measurements at 4.5 K in a maximum applied magnetic field of 2 T.

R in $RFe_{10}Mo_2$	B_c (T)		M_r ($A\ m^2\ kg^{-1}$)	
	ZFC	FC	ZFC	FC
Y	0.086	0.084	21.5	24.8
Sm	0.260	0.260	76.0	76.0
Gd	> 0.010	> 0.010	8.5	8.5
Tm	0.320	0.320	22.8	26.4
Lu	0.150	0.240	17.0	27.0

4. Mössbauer spectra of $TmFe_{10}Mo_2$

The 'window' of time observation in a ^{57}Fe Mössbauer experiment (10^{-8} s) falls in a very useful range for observation of local spin fluctuations which directly affect the effective hyperfine field H_{eff} ($\sim \langle S \rangle$) on the nucleus of ^{57}Fe . $TmFe_{10}Mo_2$ has been selected for the study of the observed transitions with Mössbauer spectroscopy, because it exhibits two well separated transitions in the thermomagnetic measurements. The alloys with $R = Ho$ and Er seems to undergo the same type of MPT showing progressively clear separation of the magnetic phases as T_C decreases with heavier R .

The observed absorption spectra as a function of temperature are plotted in figure 6 together with the distribution of H_{eff} obtained from the fitting procedure for every T . It is remarkable that the observed distributions of the hyperfine fields are nearly continuous for $T < 100$ K and present very strong relaxation effects for the temperatures $T_C > T > 110$ K. For the analysis a model with a Gaussian distribution of the H_{eff} has been applied [21] in a similar way as used for the study of Fe-Ni Invar alloys [17]. The range of small H_{eff} in the spectrum is attributed to paramagnetic states and the higher H_{eff} to ferromagnetic components. Each of the two regions is described with a distribution of H_{eff} which corresponds to a Gaussian function. The percentage f_x of the ferromagnetic components, the half-width Γ_p of the paramagnetic Gaussian function, the hyperfine H_0 at the maximum of the ferromagnetic distribution and the upper limit $H_0 + H'$ are the parameters necessary for the fitting. To every H of the ferromagnetic field distribution corresponds a six-line subspectrum with Lorentzian shaped lines. The isomer shift has been kept the same for all the components, and for the quadrupole interactions we have considered two different parameters for the paramagnetic and ferromagnetic components.

The temperature dependences of the average $\langle H_{eff} \rangle$ and f_x values obtained are plotted in figures 7 and 8, respectively. A decrease in $\langle H_{eff} \rangle$ at 110 K is shown, which coincide with the 'valley' observed in the thermomagnetic curves of the AC and DC magnetic measurements. A detailed discussion of the relaxation effects observed has been given in [21].

5. Discussion and conclusions

A variety of magnetic transitions have been observed for all $RFe_{10}Mo_2$ compounds (with an exception for $R = Gd$) as a function of temperature. The strength of R-(Fe, Mo) magnetic coupling, determined from the observed T_C , decreases more rapidly in the range of heavy rare earths (from the left to the right of the R series) compounds with the usually obtained variation in the R-Fe systems [18]. In the molecular- or mean-field approximation, T_C

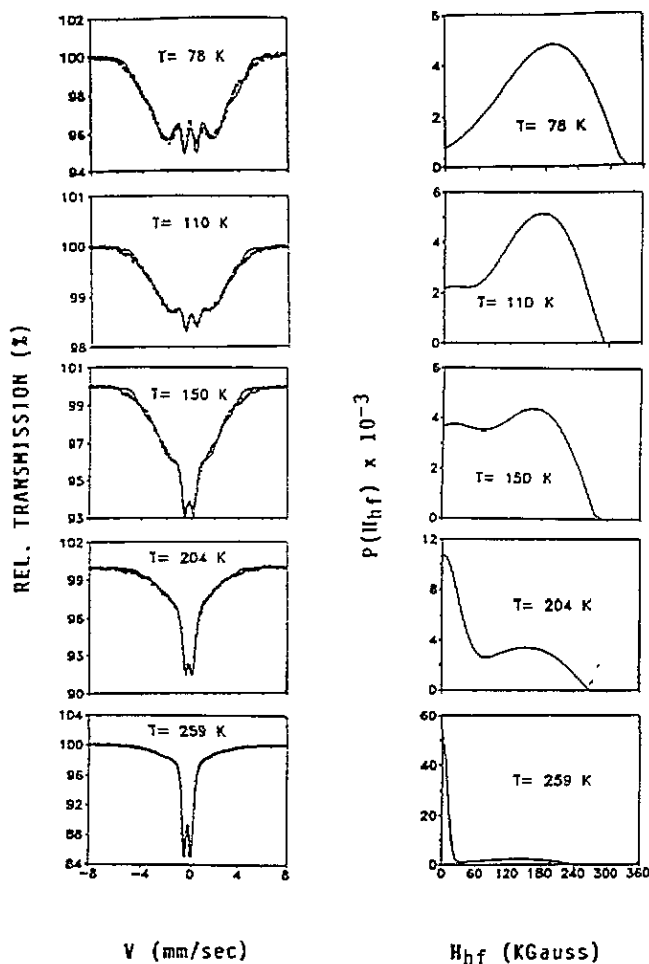


Figure 6. ^{57}Fe Mössbauer observed spectra and best fits (—) from a model with a Gaussian distribution of the magnetic hyperfine fields H_{hf} . The distribution of H_{hf} obtained as a function of temperature is shown on the left.

directly depends on the Fe–Fe and R–Fe exchange interactions (R–R exchange is usually negligible):

$$T_C \sim \frac{1}{2} [T_{\text{Fe}} + (T_{\text{Fe}}^2 + 4T_{\text{RFe}}^2)^{1/2}]$$

with $T_{\text{Fe}} = n_{\text{FeFe}} C_{\text{Fe}}$ and $T_{\text{RFe}} = n_{\text{RFe}} [2(g_j - 1)g_j](C_{\text{R}} C_{\text{Fe}})^{1/2}$, where C is the Curie constant: $\chi = C/T$. For a better understanding of the MPTs observed, it is instructive to divide this series of 1:12 alloys in two magnetic subsystems.

(a) The $\text{RFe}_{10}\text{Mo}_2$ alloys with relatively high n_{RFe} mean-field coefficients, including R = Nd, Sm, Gd, Tb and Dy, present a magnetic behaviour as a function of T which is expected from the magnetic anisotropy of the ferromagnetically or ferrimagnetically ordered 1:12 compounds.

(b) The continuous decrease in T_C through the heavy R (= Ho, Er and Tm) is remarkable and is accompanied by a number of MPTs at lower T . The observed MPTs are evidence

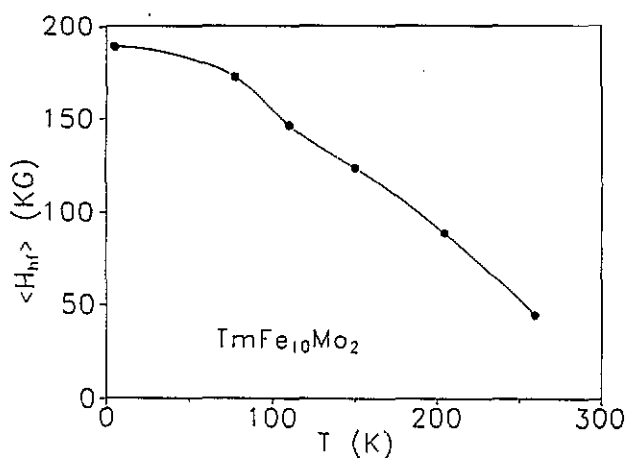


Figure 7. Thermal variation in the average magnetic hyperfine field $\langle H_{hf} \rangle$.

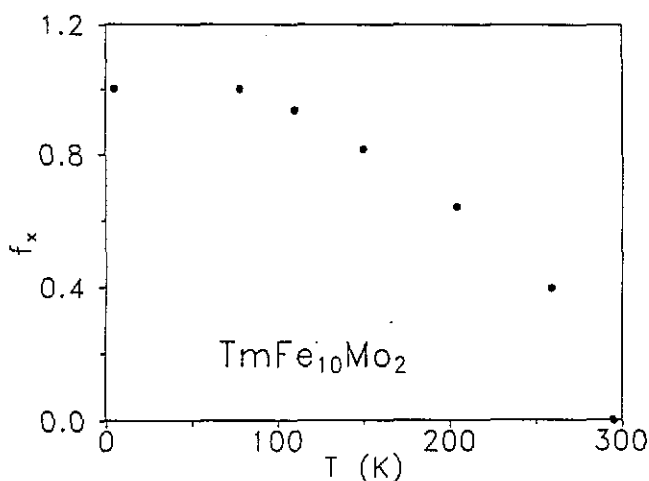


Figure 8. Temperature dependence of the fraction f_x of ferromagnetic components in the distribution of the observed effective hyperfine fields.

that the magnetic system progressively evolves, as a function of R , from a long-range magnetically ordered state to a magnetic configuration with a finite correlation length. The different magnetic interactions caused by the R atoms in the Fe–Mo magnetic environment perhaps correspond to the magnetic phase diagram proposed for systems with ‘mixed’-exchange interactions [19], in the range of exchange distributions J/Δ which separate the ferromagnetic region from the ‘strongly correlated spin-glass’ region [20]. The source of competing positive and negative exchange interactions in the above-mentioned model can be attributed to the following:

(i) a drastic change in the electronic density of states around the Fermi level, caused by the incorporation of extra Mo 4d orbitals [5], which gives an itinerant character to the band

ferromagnetism of the Fe–Mo sublattice for the concentration of Mo examined;

(ii) a significant distribution of Fe–Fe and Fe–Mo interatomic distances around the critical value of 2.5 Å [21] which may lead to local variations in the sign of exchange integrals between 3d orbitals, by considering that the magnetic interactions follow the Slater–Néel curve for transition-metal alloys [22].

In support of (ii), it has been found that nitrogenation of these compounds, which increases the unit-cell volume by approximately 3%, produces a significant increase in T_C [9]. Magnetic measurements reveal the disappearance of the MPTs observed for non-nitrogenated compounds.

Finally, the enhanced effect of the observed uncommon magnetic properties with the electronic filling of 4f states for heavy R^{3+} ions can be explained by the reduction in their ionic radii, which induces a decrease in the R–(Fe, Mo) indirect exchange interactions for heavier R [18]. Therefore, different R–Fe exchange interactions in the $RFe_{10}Mo_2$ magnetic system, as a function of R, progressively cross the ill-defined phase boundary between long-range ordered (ferromagnetic) and strongly correlated states with a finite correlation length [20]. The magnetic properties observed for the compounds with non-magnetic R = Y and Lu also support this explanation [21]. The present data reveal that the iron-rich $RFe_{10}Mo_2$ alloys provide a unique crystalline system for studying the effects of frustration on magnetic ordering. In particular, the effect of the indirect R–Fe exchange coupling for the formation of long-range magnetic order in a system with strong time relaxation effects can be examined in detail. In this respect, the present results must be considered as preliminary. To identify the specific magnetic configurations of the observed MPTs, further experiments with single crystals are required.

References

- [1] Buschow K H J and de Mooij D B 1990 *Commission of European Communities CEAM Final Report* p 63
- [2] Muller A 1988 *J. Appl. Phys.* **69** 249
- [3] Hu Bo-Ping, Li Hong-Shuo, Coey J M D and Gavigan J P 1990 *Phys. Rev. B* **41** 2221
- [4] Christides C, Anagnostou M, Li Hong-Shuo, Kostikas A and Niarchos D 1991 *Phys. Rev. B* **41** 2181
- [5] Christides C, Li Hong-Shuo, Kostikas A and Niarchos D 1991 *Physica B* **175** 329
- [6] Verhoef R, de Boer F R, Zhang Zhi-dong and Buschow K H J 1988 *J. Magn. Magn. Mater.* **75** 319
- [7] Koestler C, Shultz L and Thomas G 1990 *J. Appl. Phys.* **67** 2532
- [8] Shultz L, Schnitcke K and Wecker J 1990 *J. Magn. Magn. Mater.* **83** 254
- [9] Anagnostou M, Christides C and Niarchos D 1991 *Solid State Commun.* **78** 681
- [10] Anagnostou M, Christides C, Pissas M and Niarchos D 1991 *J. Appl. Phys.* **70** 6012
- [11] Kou X C, Christides C, Grossinger R, Kirchmayr H R and Kostikas A 1992 *J. Magn. Magn. Mater.* **105–7** 1341
- [12] Christides C, Kostikas A, Niarchos D and Simopoulos A 1988 *J. Physique Coll. Suppl.* **12** 49 539
- [13] Chikazumi S 1964 *Physics of Magnetism* (New York: Wiley)
- [14] Stefanski P, Kowalczyk A and Wrzeciono A 1989 *J. Magn. Magn. Mater.* **81** 155; 1989 *J. Magn. Magn. Mater.* **82** 125
- [15] Li Hong-Shuo and Coey J M D 1991 *Handbook of Magnetic Materials* vol 6, ed K H J Buschow (Amsterdam: North-Holland) p 1
- [16] Li Hong-Shuo, Hu Bo-Ping, Gavigan J P, Coey J M D, Pareti L and Mose O 1988 *J. Physique Coll. Suppl.* **12** 49 541
- [17] Shimizu M and Kobayashi H 1984 *J. Phys. Soc. Japan* **53** 2111
- [18] Belorizky E, Fremy M A, Gavigan J P, Givord D and Li Hong-Shuo 1987 *J. Appl. Phys.* **61** 3971
- [19] Gabay M and Toulouse G 1981 *Phys. Rev. Lett.* **47** 201
- [20] Ryan D H, Strom-Olsen J O, Provencher R and Townsend M 1988 *J. Appl. Phys.* **64** 5787
- [21] Christides C, Kostikas A, Zouganelis G, Psycharis V, Kou X C and Grossinger R 1993 *Phys. Rev. B* **47** 11 220
- [22] Néel L 1936 *Ann. Phys., Paris* **5** 232